Interaction between Structural Walls, Flooring Slab and Gravity Columns

R.E. Sedgh[1], R.P. Dhakal[1], A.J. Carr[1,2] & C.L. Lee[1]

1.*Department of Civil Engineering, University of Canterbury, Christchurch, New Zealand*

2.*MC Consulting Engineers, Christchurch, New Zealand*

2017 NZSEE Conference

ABSTRACT: In multi-story shear wall buildings with gravity columns and slabs, structural walls serve as main lateral force resisting elements while the columns and concrete flat slabs (in-situ or post-tensioned) are only designed to carry gravity loads. However, the gravity system is required to have deformation compatibility with the lateral force resisting system. It is a common practice to assess seismic performance of the whole structural system based on the seismic behavior of isolated structural walls mainly because slabs and gravity columns have very low elastic lateral stiffness compared with the in-plane stiffness of structural walls. To scrutinize the effect of interaction between structural walls and gravity frames (via slabs), in this study, nonlinear static analyses are conducted on various prototype shear wall buildings and their responses are predicted. The system over-strength of prototype buildings with different slab properties is examined. It is found that the wall, frame and slab interaction can induce substantial over-strength in the system, which can increase the shear demand on the structural walls. A simplified procedure to estimate the system over-strength is proposed in this paper.

1. INTRODUCTION

In typical structural design practice, because the performance of lateral-load-resisting systems is the main focus of (nonlinear) lateral analysis, floor systems are considered only as a source of mass and gravity loads. Therefore, the contribution of the floor systems (such as two-way in-situ or post-tensioned flat slabs) to the overall stiffness or strength of the building is often neglected.

Bertero et al., (1984) performed shaking table tests on a 1/5 scale and a full scale multi-storey shear wall-frame building. Following these system-level testing, significant contribution of the flooring system (two-way slabs) to the ultimate lateral strength of the building was confirmed. They stated that the axial growth and rocking of the structural wall at its base (due to neutral axis movement) caused activation of a three-dimensional outrigging action in the surrounding space frames. This phenomenon was called three-dimensional effects. The induced outrigging action of the space frames should be accounted for in the design process. This phenomenon introduces extra over-strength to the system and it is highly dependent on the level of drift which can be achieved at ultimate limit state. Therefore, it has been called kinematic over-strength. Restrepo et al. (2007) also conducted another experimental investigation comprising of shake table tests of a slice of a multi-storey shear wall building including slabs and gravity columns. The authors noted that the main source of system base moment resistance in Westward direction at the DBE level shaking included three major components: i) 55% from the web wall moment capacity ii) 32% due to coupling of the web through the slotted slabs iii) 10% due to axial force in the perpendicular gravity columns. However, in real practice, a precise estimation of the over-strength in multi-storey buildings is difficult since many factors are contributing to it. According to FEMA 450 (2003), the basic components of structural over-strength (Ω_0) consists of material over-strength (Ω_M), system over-strength (Ω_S), and design over-strength (Ω_D).These components of over-strength are presented schematically in Figure 1. This study focuses on addressing the effect of structural wall-slab-gravity column interaction on the system over-strength (Ω_S) factor in typical multi-storey shear wall buildings. System over-strength (Ω_S) is the ratio of the ultimate lateral force the structure is capable of resisting, F_n in Figure 1, to the actual force at which first significant yield occurs, F_2 in Figure 1. It is dependent on the amount of redundancy contained in the structure as well as any probable contribution of secondary components in resisting lateral force. Re-distribution of internal actions after ductile yielding in critical zones is another key parameter.

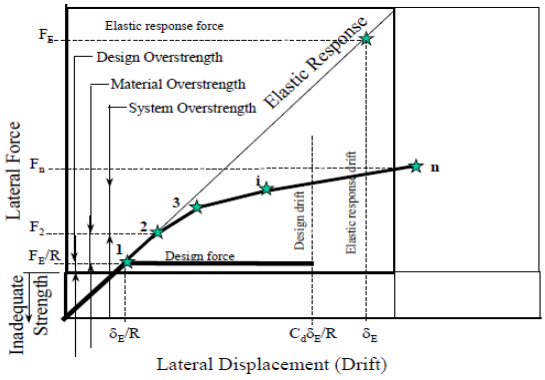

Figure 1. Factors affecting over-strength of a building (FEMA 450)

The fundamental objective of the current design practice and capacity design of structural wall buildings is that energy is dissipated through the formation of plastic hinges at the base of shear walls while floor diaphragms remain elastic. The flooring system is vertically supported by a combination of shear walls and gravity resisting columns. The effects of over-strength are not always beneficial in capacity design. For example, the flexural over-strength of members leads to increased shear forces when plastic hinges forms which may result in non-ductile failure (Park, 1996). Therefore, any possible source of over-strength in a building should be taken into consideration in capacity design.

This paper attempts to investigate the system over-strength in multi-storey RC wall buildings with slabs in five cases of lateral-load-resisting systems: (i) case 1 has concrete structural walls only (zero out of plane flexural stiffness of slabs); and (ii) the remaining four cases have rectangular shear walls with slabs having different section flexural stiffness and/or varying bay lengths. This study intends to investigate the effects of bay length and out-of-plane sectional stiffness of slabs on the system over-strength factor of shear wall buildings in the direction of walls in-plane. This study also proposes a simplified method to account for the over-strength factor in design. It also presents the results from a finite element analysis and discusses the influence of modeling RC slab elements on the predicted performance of shear wall buildings.

2. MECHANISM RELATED TO WALL-FRAME-SLAB INTERQACTION

This section explains the mechanism related to the wall-frame-slab interaction in the post-elastic phase. An eight-story building with a floor plan of 30 m by 18 m is used as the reference building. Typical floor plan of the multi-storey shear wall building, the wall section and the design information are illustrated in Figure 2. The gravity system of the building consists of 200 mm thick RC slabs and circular (500 mm diameter) RC columns. Five cases are used in this study; the same structural wall thickness is used in all cases. Typical story height is assumed to be 3.20 meter. The building is designed based on the design provisions defined in the NZ concrete structures standard (NZS3101-2006) and the NZ loading standard (NZS1170.5-2004).

The deformation patterns of the whole system in the linear and non-linear phase are demonstrated in Figure 3. These figures illustrate only the system behavior in Y direction indicated in the building floor plan. Figure 4 also shows a schematic deformation of a representative flooring system due to rocking of an attached structural wall cross-sectional deformation. The connection between the flooring system and the structural walls significantly differs in construction practice due to variability in the flooring types. However, in this study typical rigid connection is assumed.

For a given applied force pattern over the building height, tensile edge elongation or compression edge shortening of structural walls in the post-elastic response (due to the movement of neutral axis in monotonic loading and elongation (axial growth) of the wall in cyclic loading) triggers out-of-plane stiffness of the slabs (or other roofing/flooring systems). This interaction induces additional axial forces in the gravity columns, which can develop extra moment capacity in the system. In a ductile structure, roofing system (or flat floor slabs in this case study) will almost always be required to remain elastic, so that they can sustain their function of transferring forces to the main lateral load resisting elements,

and tying the building together. Therefore, diaphragms (slabs) should in principle have the strength to sustain the maximum forces that may be induced in them for a chosen yielding mechanism within the rest of the structure.

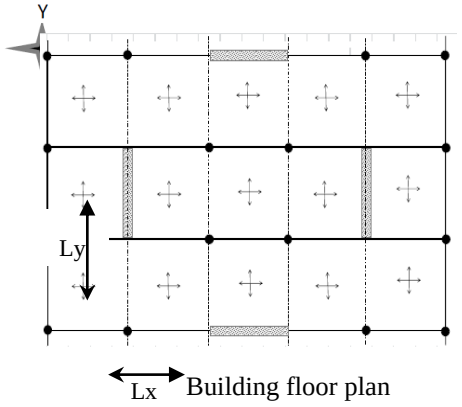

Building floor plan

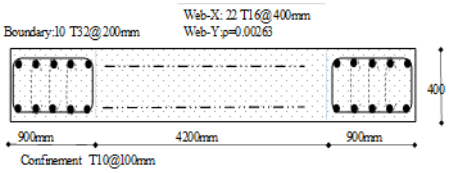

Wall base section

Rectangular wall section	6000 x 400 mm	Near fault factor	1
Typical floor height	3.20 m	Seismic weight on each wall(base)	4542.3 kN
f_c	30 MPa	Soil type	D
f_{yl}, f_{yh}	430 MPa , 300 MPa	Near fault factor	1.0
Gravity columns dimension	D500 mm	Zone factor	0.4
Slab thickness	200 mm	Return period factor	1.0
Gravity load on each wall(base)	$0.08f_cA_g$	Structural ductility	5

Design information

Figure 2. Building plan, wall section and design information

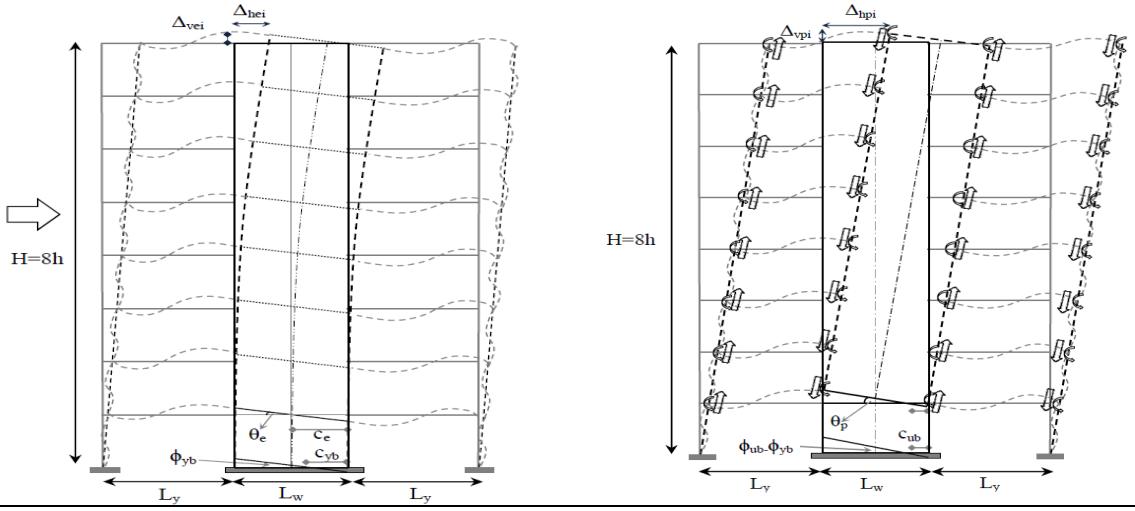

Figure 3. a) Elastic deformation due to elastic curvature b) Plastic deformation due to plastic hinge rotation

H: Building height
h: Storey height
L_w: Wall length
L_y: Column distance to wall edge in Y direction

c_e : Center of section rotation (elastic)
c_{yb} : Base section neutral axis depth at effective yield
c_{ub} : Base section neutral axis depth at ultimate
θ_{ei}: Rotation of storey level at effective yield
θ_p: Plastic rotation of base and storey level

Δ_{vei}: Vertical displacement of tension edge at effective yield
Δ_{vpi}: Plastic vertical displacement of tension edge
ϕ_{yb}= ϕ_{yeff} Base effective yield curvature
ϕ_{ub}: Base ultimate curvature

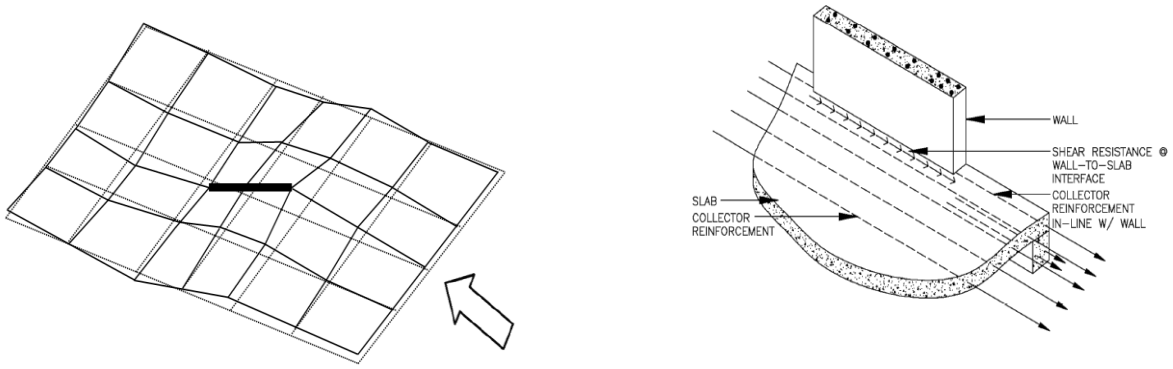

Figure 4. a) Deformation compatibility of wall and surrounding slabs in a typical floor b) slab to wall connection

2.1. Distribution of curvature over the height

When the wall base section curvature reaches effective yielding curvature (equivalent to yielding of all reinforcement in the boundary element of the wall base section), the distribution of curvature over the height of the structural wall can be found at each story level by employing elastic theory. In this work, a continuous lateral load pattern with zero intensity at the base has been assumed over the building. The deformation pattern of a prismatic rectangular cantilever wall with constant flexural stiffness can be obtained satisfying the geometric and force boundary conditions. Hence, the inter-relation between the roof deformation and the base curvature can be established as a function of building height and a constant coefficient as:

$$\Delta_{roof} = \frac{11H^2}{40} \emptyset_{base} \quad (1)$$

It is also possible to find generic equations for the curvature and the rotation distribution over the height in terms of base curvature as a function of floor distance from the base (Z), which can be expressed as:

$$\emptyset(Z) = \frac{M(Z)}{EI(Z)} = \frac{\emptyset_{base}}{2H^3} Z^3 - \frac{3\emptyset_{base}}{2H} Z + \emptyset_{base} \text{ , } \theta(Z) = \frac{\emptyset_{base}}{8H^3} Z^4 - \frac{3\emptyset_{base}}{4H} Z^2 + \emptyset_{base} Z \quad (2)$$

Therefore, the distribution of curvature and distribution of rotation in each storey level over the wall height (in each storey level) can be estimated by employing Equation (2) when the curvature at base section reaches the effective yield curvature. It is important to highlight that in a real multi-storey shear wall building the lateral load distribution is a discrete function over the building height. Hence, a correction factor is defined to adjust Equation (1) based on number of stories (n). Thus, the modified form of Equation (1) including the correction factor α (which is a function of the number of stories) turns out to be:

$$\Delta_{roof} = \frac{11H^2}{40} \emptyset_{base} \times \alpha \qquad \alpha = 0.835n^{0.0465} \quad (3)$$

Given the fact that most multi-storey shear wall buildings commonly have 5 storeys and more, the application of Equation (1) induces a maximum of 10% error in the calculation, which is justifiable for practical purpose.

2.2. Estimation of effective yield curvature and neutral axis depth

An extensive parametric section-analysis is conducted to find the variation of effective yield curvature (and equivalent neutral axis depth) in the moment- curvature diagram. Moreover, the parametric study also investigates the variation of neutral axis depth when the section reaches its ultimate flexural strength. The effective yield curvature is determined using standard moment-curvature analyses. Although the realistic effective yield curvature of a section can change slightly due to tension stiffening of RC concrete, diagonal cracks and reinforcement bar slip, this study neglects them. The effective yield curvature, ϕ_{yeff}, is obtained from extrapolating the first-yield curvature, ϕ_y to a point where the moment reaches ultimate strength, M_u, assuming elasto-plastic response, or

$$\phi_{yeff} = (M_u/M_y)*\phi_y \quad (4)$$

where M_y is the moment resistance when first longitudinal rebar located in the boundary zone reaches ε_y and M_u is the ultimate (nominal) flexural strength, defined as the moment resistance corresponding to a concrete strain of 0.003 at the extreme compression fiber.

Charts are generated to allow rapid estimation of the effective yield curvature of rectangular wall cross sections for a given axial force and section geometry. A typical chart is given in Figure 5 for a rectangular cross section. Also, Figure 6 displays the normalized neutral axis depth (measured from the extreme compression fiber to the neutral axis) when the section reaches its ultimate strength. It is evident from Figure 6 that the value of c_{ub}/L_w varies from 0.08 to 0.2 depending on boundary zone reinforcement and wall lengths for the range of axial forces considered here. However, the normalized neutral axis depth is insensitive to wall length

2.3. Estimation of vertical deformation of wall edges

Figure 7 demonstrates the detailed procedure to estimate the wall edge deformations in elastic and plastic states. The vertical deformation of wall at tension (left) and compression (right) side edges are

determined in each story level. Plastic deformation of wall edges due to plastic rotation at the base section is presented in Figure 7(b). The total tension (upward) or compression (downward) deformation of wall edges is equal to $\delta_{ti}=\Delta_{vei}+\Delta_{vpi}$ where δ_{ti}, Δ_{vei} and Δ_{vpi} represent the total vertical deformation, the elastic vertical deformation and the plastic vertical deformation of the wall edge at storey i, respectively. In the proposed procedure shown in Figure 7, the wall edge vertical plastic deformations (denoted as Δ_{vpi}) are estimated based on the value of base plastic rotation (θ_p), neutral axis depth (c_{ub}) and floor distance from the base (h_i). The appropriate value of the base plastic rotation highly depends on appropriate selection of equivalent plastic hinge length and ultimate curvature. It will be discussed in the next section.

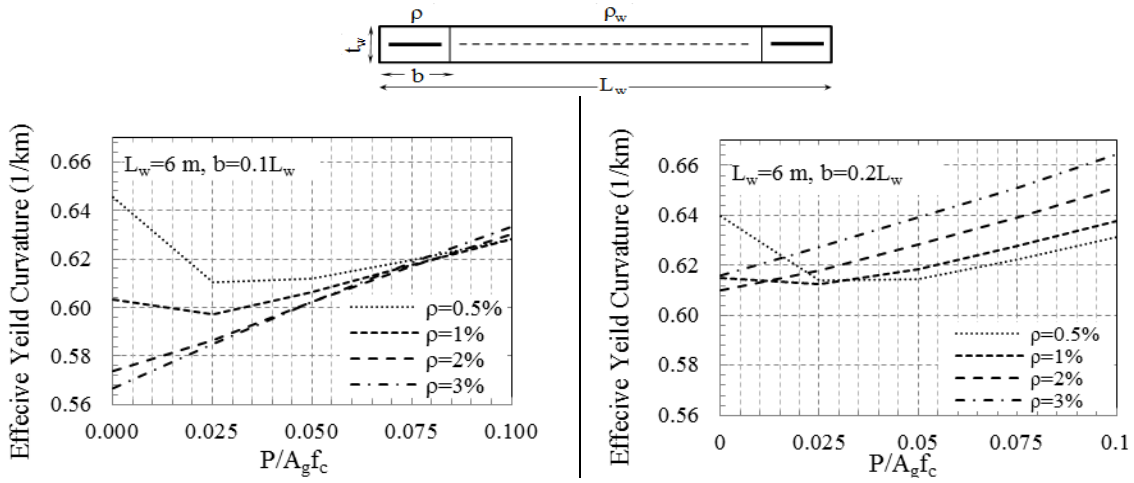

Figure 5. Variation of effective yield curvature with different parameters

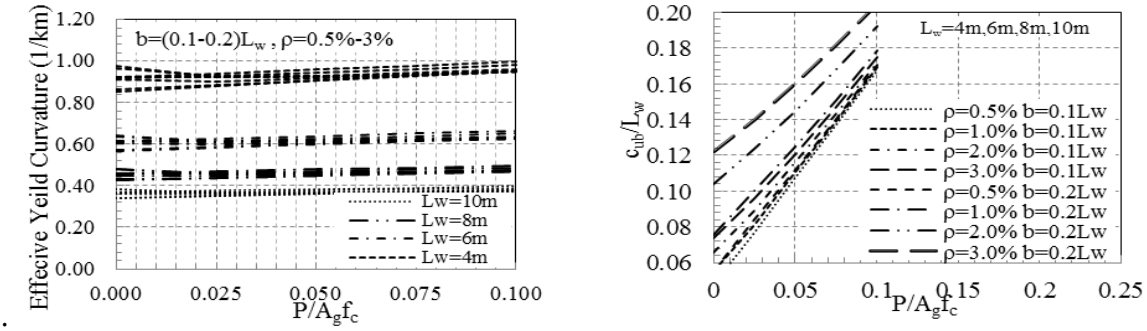

(a) (b)

Figure 6. a) Effect of wall length on effective yield curvature b) Variation of neutral axis depth with different parameters at maximum flexural strength

2.4. Slabs Contribution

To simplify the hand calculation method, two-way slabs in each floor should be replaced with an equivalent elastic beam of an effective width. In a real structure, deformation compatibility of slabs with the cross-sectional rotation of the wall causes not only bending in each direction (curvature in both directions) but also torsional warping. However, we assume zero torsional stiffness for slabs to derive a simple hand calculation method. It is assumed that the equivalent width of slabs is equal to the bay length in each direction. Neglecting the contribution of axial force in the corner columns is another assumption which has been adopted in this study. By assuming a low flexural stiffness for gravity columns, the sub-assemblage which is representing slabs with an effective width can be replaced with a beam with a pin on the far end from the wall. The vertical deformations as well as cross-sectional rotation are prescribed as boundary conditions on the other end of equivalent beam where it is connected to the wall.

2.5. Maximum moment capacity of the system

Replacing z with the variable h_i and $\varphi_{base}=\varphi_{yeff}$ in Equation (2), Equation (5) is obtained which gives the

elastic rotation of each storey.

$$\theta_{ei}(z = h_i) = \left(\frac{\varphi_{yeff}}{8H^3} h_i^4 - \frac{3\varphi_{yeff}}{4H} h_i^2 + \varphi_{yeff} h_i\right) \quad (5)$$

The total rotation of each storey (θ_i) is the summation of elastic rotation and plastic rotation in each floor level. Plastic rotation of all stories is equal to the plastic rotation at the base. However, the corresponding vertical plastic deformation in each storey is different.

$$\theta_i = \theta_{ei} + \theta_p \qquad \theta_p = (\varphi_u - \varphi_{yeff}) \times l_p \quad (6)$$

Plastic rotation of the base can be found from the simplified plastic hinge analysis method (Equation (6) above). This equation uses the already established effective yield curvature (φ_{eff}) formulation; it needs an experimentally derived equivalent plastic hinge length (l_p) and ultimate usable curvature of the base section (φ_u).

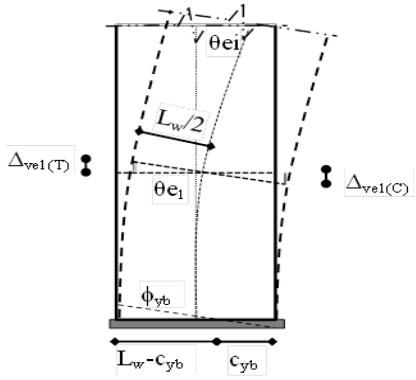

a) Edge deformation when the base curvature reaches the effective yield

Steps to estimate the deformation of wall edges at effective yielding

1) Calculate the effective yield curvature at the base section using Equation 4 (or Figure 5)

2) Calculate the rotation distribution at storey level using Equation 5

3) Calculate the wall edge deformation as:

$\Delta_{ve1(T)} = \Delta_{ve1(C)} = (L_w/2).\theta_{e1}$ storey 1

$\Delta_{vei\,(T)} = \Delta_{vei\,(C)} = (L_w/2).\theta_{ei}$ storey i

$\Delta_{vei(T)}$, $\Delta_{vei(C)}$: Tension and Compression edge upward and downward deformation

θ_{ei}: Rotation at storey level i

L_w: Wall length

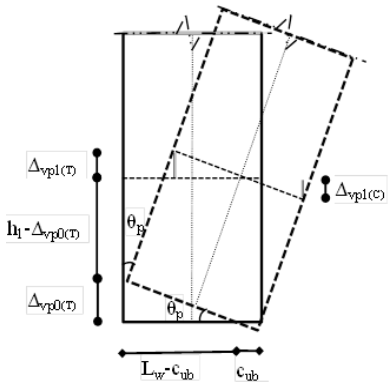

b) Edge plastic deformation

Steps to estimate the plastic deformation of wall edges

1) Calculate the effective yield curvature at the base section using Equation 4 (or charts)

2) Calculate the ultimate usable curvature by NZS3101-2006 provision and plastic hinge length equal to $0.3L_w$

3) Calculate the neutral axis depth (C_{ub}) at the maximum flexural strength by moment-curvature analysis or use the chart proposed in Figure (6b):

4) Calculate the wall edge plastic deformation

$\Delta_{vp0(T)} = (L_w - c_{ub}).\theta_p$ $\Delta_{vp0(T)} = (c_{ub}).\theta_p$ base

$\Delta_{vpi(T)} = \Delta_{vp0(T)} - h_i.(1-\cos\theta_p)$ storey i

$\Delta_{vpi(C)} = \Delta_{vp0(C)} - h_i.(1-\cos\theta_p)$ storey i

$\Delta_{vpi(T)}$, $\Delta_{vpi(C)}$: Tension and Compression edge upward and downward plastic deformation

θ_p: Plastic hinge rotation

C_{ub}: Neutral axis depth at maximum flexural strength

h_i: Storey i height from the base

Figure 7. Steps to estimate the elastic and plastic deformation of wall edges

To find the cross-sectional rotation of a structural wall in each floor of a multi-storey building and the corresponding vertical deformation of wall edges due to arbitrary lateral force, we can use Equation (5) and Equation (6) along with the procedure presented in Figure (7) which results in the following expressions for the wall edges total vertical deformation in tension and compression side:

$$\delta_{ti} = \left(\frac{\varphi_{yeff}}{8H^3} h_i^4 - \frac{3\varphi_{yeff}}{4H} h_i^2 + \varphi_{yeff} h_i\right) \times \left(\frac{L_w}{2}\right) + (L_w - c_{ub}) \times \theta_p - h_i(1 - cos\theta_p) \quad (7)$$

$$\delta_{ci} = \left(\frac{\varphi_{yeff}}{8H^3} h_i^4 - \frac{3\varphi_{yeff}}{4H} h_i^2 + \varphi_{yeff} h_i\right) \times \left(\frac{L_w}{2}\right) + (c_{ub}) \times \theta_p - h_i(1 - cos\theta_p) \quad (8)$$

δ_{ti} and δ_{ci} are the total wall edge vertical deformation due to total sectional rotation of the structural wall

in each floor in tension and compression side respectively. Figure 8 illustrates the application of those deformations as an enforced boundary condition on the equivalent beams in Y and X directions. The beam to the gravity columns connections are treated as a pin end without any vertical flexibility. It implies that axial deformation due to induced axial force in gravity columns is overlooked.

Figure (8b) demonstrates the schematic spatial representation of actions induced in the gravity columns. They generate additional storey moments in the each storey. This extra moment capacity is obtained by multiplying the axial force in the columns by their distance from center of wall section.

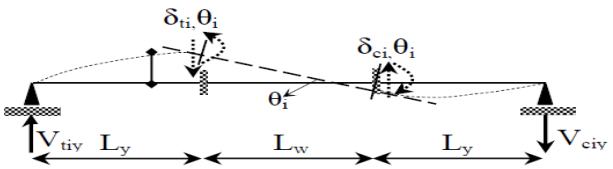

Equivalent beam in Y direction (storey i)

(a)

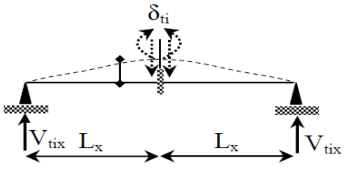

Equivalent slab in X direction (tension side) (storey i)

(a)

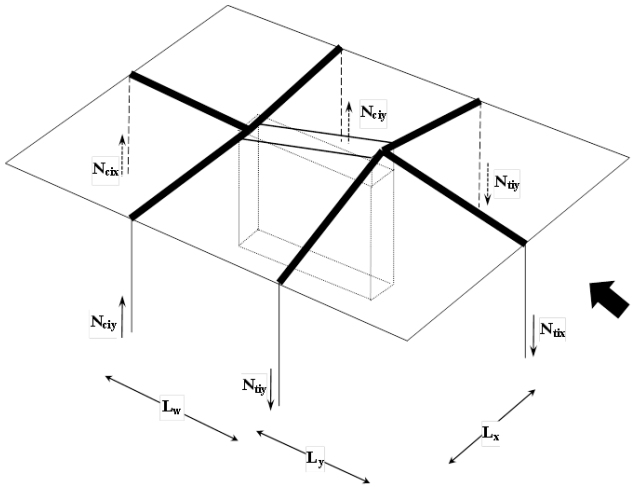

(b)

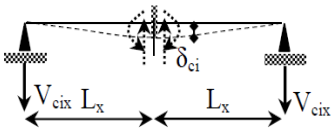

Equivalent slab in X direction (compression side) (storey i)

(a)

Figure 8. a) Enforced boundary conditions on equivalent beams b) Induced axial forces in gravity columns

Figure 9 presents step by step procedure to find the induced actions in gravity columns due to the enforced boundary conditions on the equivalent beams. The proposed procedure accounts for the different boundary conditions in each storey level. The induced actions in tension and compression side of structural walls are estimated separately. The summation of all storey moments gives the total base moment resistance of the system as indicated in Equation (9)

$$\sum_{i=1}^{n} M_{col} = \sum_{i=1}^{n}\left(\frac{3EI_{eff}\delta_{ti}}{L_y^3} + \frac{3EI_{eff}\theta_i}{L_y^2}\right)(L_y + L_w/2) + \sum_{i=1}^{n}\left(\frac{3EI_{eff}\delta_{ti}}{L_x^3}\right)\left(\frac{L_w}{2}\right) \times 2 + \sum_{i=1}^{n}\left(\frac{3EI_{eff}\delta_{ci}}{L_y^3} + \frac{3EI_{eff}\theta_i}{L_y^2}\right)(L_y + L_w/2) + \sum_{i=1}^{n}\left(\frac{3EI_{eff}\delta_{ci}}{L_x^3}\right)\left(\frac{L_w}{2}\right) \times 2 \quad (9)$$

This additional moment capacity of the system at ultimate limit state can be normalized to the nominal wall flexural strength in order to establish the system over-strength as below:

$$\Omega = \frac{M_{wall-nominal} + M_{wall-hardening} + \sum_{i=1}^{m} M_{col}}{M_{wall-nominal}} \quad \Omega = 1 + \frac{M_{wall-hardening}}{M_{wall-nominal}} + \frac{\sum_{i=1}^{n} M_{col}}{M_{wall-nominal}} = 1.25 + \frac{\sum_{i=1}^{n} M_{col}}{M_{wall-nominal}} \quad (10)$$

$$\Omega = 1 + \frac{M_{wall-hardening}}{M_{wall-nominal}} + \frac{\sum_{i=1}^{n} M_{col}}{M_{wall-nominal}} = 1.25 + \frac{\sum_{i=1}^{n} M_{col}}{M_{wall-nominal}} \quad (11)$$

This normalization is adopted in the hand calculation method. However, in the finite element analysis, additional flexural strength due to strain hardening can be automatically included in the model by employing material laws with strain hardening of rebar and confinement effect of concrete. To compare

in a consistent manner, the value of material over-strength in hand calculation is assumed 25% higher than nominal flexural strength of walls. This procedure implies a consistent comparison between the finite element method and the simplified method.

1) Calculate effective width of slabs in X and Y direction respectively : L_x and L_y
2) Calculate shear force induced in the equivalent slab element in X direction at storey i:
$V_{tix}= (3EI_{eff}* \delta_{ti}/L_x^3)$, $V_{tix}= (3EI_{eff}* \delta_{ci}/L_x^3)$
3) Calculate shear force induced in the equivalent slab element in Y direction at storey i:
$V_{tiy}=(3EI_{eff}*\delta_{ti}/L_y^3+3EI_{eff}*\theta_i/L_y^2)$, $V_{ciy}=(3EI_{eff}*\delta_{ci}/L_y^3+3EI_{eff}*\theta_i/L_y^2)$
4) Calculate total axial force in the storey columns in X direction:
$N_{tix}=\sum V_{tix}$, $N_{tix}=\sum V_{tix}$
5) Calculate total axial force in the storey columns in Y direction:
$N_{tiy}=\sum V_{tiy}$, $N_{ciy}=\sum V_{ciy}$
6) Calculate the storey moment of system due to axial force in the storey columns in X direction:
$M_{tix}= N_{tix} *(L_w/2)$, $M_{cix}= N_{cix}*(L_w/2)$
7) Calculate the storey moment of system due to axial force in the storey columns in Y direction:
$M_{tiy}= N_{tiy} *(L_y+L_w/2)$, $M_{ciy}= N_{ciy} *(L_y+L_w/2)$
8) Calculate the total storey moment of system due to axial force in the storey columns:
$M_{tit}(T)= M_{tix} + M_{tiy}$,
$M_{cit}(C)=M_{cix} + M_{ciy}$,
$M_i = M_{tit}(T) + M_{cit}(C)$

Figure 9. Proposed steps to calculate the induced actions due to deformation compatibility in each floor

3. HAND CALCULATION METHOD

The proposed simplified formulation is applied to a building prototype with the same slab length in two directions equal to 6 m and effective flexural stiffness equal to 0.25EIg which later has been named case 2. Due to space limitation, the detailed information of hand calculation procedure is shown only for case 2 in Table 2, Table 3 and Table 4.

3.1. Estimation of the wall edges vertical deformation and sectional rotation

The curvatures, elastic rotations, base plastic rotation and corresponding wall edges vertical deformation of the wall in each story level of the prototype building are calculated by employing the proposed method. The calculated values are shown in Table 2. In the following section, five more prototype buildings are analyzed to scrutinize the earlier explained three-dimensional spatial effects of slabs on the system behavior.

3.2. Calculation of induced actions

In this section, based on the values calculated for the vertical deformation of wall edges in tension and compression side as well as sectional rotation (Table 2), the induced actions are calculated in each storey by employing method proposed in Figure 9. Table 3 presents the value of axial force and their corresponding moments in each storey level. Table 4 summarizes the total base moment in each storey level and it is shown that the system-over strength is equal to 1.7 for this particular system.

4. FINITE ELEMENT MODELLING

Three-dimensional nonlinear finite element models are built using SAP2000 (CSI, 2014) for the prototype buildings to obtain their capacity curves. The seismic mass at all floors was assigned as distributed mass on walls. A rigid diaphragm is incorporated by slaving the translational degrees of freedom at each floor level. The foundation of the building was assumed as rigid, and P-delta effects are taken into account.

4.1 Structural Wall Modelling

Nonlinear shell elements representing the in-plane behavior of RC panels were used to model the rectangular walls. The confined and unconfined concretes were modeled differently, but the tensile strength of concrete was neglected. Concrete stress-strain relationship was based on Mander model

(Mander et al., 1988). The steel reinforcement stress-strain was bilinear model including strain hardening from ε=0.01. Slabs are modeled as elastic shell elements with stiffness values of EI_{eff} = $0.25EI_g$ (flexural) and GA = $0.5GA_g$ (shear). All slabs are assigned a specified concrete strength of f'_c = 30 MPa. Shear modulus (G) is calculated using a Poisson's ratio ν = 0.2. The columns are modelled as elastic beam elements with very low flexural stiffness. The elastic properties of the columns are calculated using the cross-section dimensions and the stiffness modification factors; i.e. EI_{eff} = $0.01EI_g$ (flexural), GA = $1.0GA_g$ (shear). This approach can give us a transparent comparison between the models without interaction (case 1) and those with interactions (case 2-5).

Table 2. Elastic and plastic vertical displacement of wall edges for case 2

Storey section	**0 (Base)**	**1**	**2**	**3**	**4**	**5**	**6**	**7**	**8 (Roof)**
Curvature(φ_i) (1/km)	0.71	0.7105	0.7151	0.7281	0.7536	0.7957	0.8585	0.9464	1.064
Θ_{ei} (rad)	0	0.0020	0.0037	0.0049	0.0058	0.0064	0.0067	0.0068	0.0068
Δ_{vei}(T) (mm)	0	6.1787	11.1026	14.8318	17.466	19.1450	20.0486	20.3964	20.448
Δ_{vei}(C) (mm)	0	6.1787	11.1026	14.8318	17.466	19.1450	20.0486	20.3964	20.448
Θ_p(rad)	0.0192	-	-	-	-	-	-	-	-
Δ_{vpi} (T) (mm)	-	97.767	97.179	96.592	96.003	95.415	94.827	93.651	93.063
Δ_{vpi}(C) (mm)	-	16.665	16.077	15.489	14.901	14.313	13.725	13.137	12.550
δ_{ti} (mm)	-	103.35	107.694	110.835	112.881	113.972	114.288	114.048	113.511
δ_{ci} (mm)	-	22.844	27.179	30.320	32.367	33.458	33.774	33.534	32.997

Table 3. Extra moment due to induced actions in gravity columns in each storey for case 2

Tension Edge / Storey	$\delta_{i(T)}=\Delta_{vei}+\Delta_{vpi}$ (m)	θ_i (rad)	V_{tiy} (kN)	V_{tix} (kN)	$N_{tiy}=\sum(V_{tiy})$ (kN)	$N_{tix}=\sum(V_{tix})$ (kN)	M_{tiy} (kN.m)	M_{tix} (kN.m)	$M_{tit(T)}$ (kN.m)
8	0.11350	0.026	113.81	47.93	-113.81	-47.93	1024.33	287.61	371.09
7	0.11405	0.026	114.00	48.16	-227.82	-96.10	2050.34	576.60	744.95
6	0.11429	0.026	113.81	48.27	-341.63	-144.37	3074.65	866.21	1120.07
5	0.11397	0.025	112.92	48.14	-454.55	-192.51	4090.92	1155.05	1493.62
4	0.11288	0.025	111.04	47.68	-565.59	-240.19	5090.30	1441.15	1861.69
3	0.11083	0.024	107.96	46.82	-673.54	-287.01	6061.89	1722.07	2219.42
2	0.10769	0.023	103.48	45.50	-777.02	-332.51	6993.21	1995.06	2561.27
1(Total)	0.10335	0.021	97.49	43.67	-874.51	-376.18	7870.62	2257.07	2881.18
Compression Edge / Storey	$\delta_{i(C)}=\Delta_{vei}+\Delta_{vpi}$ (m)	θ_i (rad)	V_{ciy} (kN)	V_{cix} (kN)	$N_{ciy}=\sum(V_{ciy})$ (kN)	$N_{cix}=\sum(V_{cix})$ (kN)	M_{ciy} (kN.m)	M_{cix} (kN.m)	$M_{cit(C)}$ (kN.m)
8	0.0330	0.026	79.79	13.91	79.79	13.91	718.15	83.49	371.09
7	0.0335	0.026	79.98	14.14	159.78	28.06	1437.98	168.36	744.95
6	0.0338	0.026	79.79	14.25	239.57	42.31	2156.11	253.85	1120.07
5	0.0335	0.026	78.90	14.12	318.47	56.43	2866.20	338.57	1493.62
4	0.0324	0.025	77.02	13.66	395.49	70.09	3559.40	420.55	1861.69
3	0.0303	0.024	73.94	12.80	469.42	82.89	4224.81	497.35	2219.42
2	0.0272	0.023	69.46	11.48	538.88	94.37	4849.95	566.22	2561.27
1(Total)	0.0228	0.021	63.47	9.65	602.35	104.02	5421.18	624.11	2881.18

4.2 Analysis Method

Generally, the accuracy of pushover analysis in representing the structural seismic performance is debatable. However, this simple method provides a useful understanding of the expected behavior of the structures. Therefore, this study is based on the pushover analysis results. All analyses are performed with a gravity load of P=1.0D+0.25L.

Table 4. System over-strength due to interaction for case 2

Storey	M_i (total moment) (kN.m)	Ω_i
8	2113.58	
7	4233.27	
6	6350.83	
5	8450.74	
4	10511.39	
3	12506.13	
2	14404.44	
1(Total)	16172.99	1.45+0.25=1.70

4.3 Analysis Results

The simplified hand calculation method which is proposed to account for system over-strength is verified for the five different cases. The slab flexural stiffness and geometrical dimensions of these cases are listed in Table 5. Typical floor plan and geometry of prototype buildings have been already defined in the section 2 and Figure 2. In all case studies, the structural wall properties are the same while the slab bay length and/or their flexural stiffness are varied.

Table 5. Variables for different case studies

Case	slab flexural stiffness	slab length in X direction(Lx)(m)	slab length in Y direction(Ly)(m)
1	0	6	6
2	$0.25EI_g$	6	6
3	$0.25EI_g$	6	8
4	$0.25EI_g$	8	6
5	$0.50EI_g$	6	6

To scrutinize the application of the proposed simplified formula for over-strength estimation, the over-strength of above case studies is calculated by employing the simplified hand calculation method as well as finite element approach. Cases 3 and 4 are selected to represent the effect of change in length of slabs (bay) in x and y directions, respectively. The out-of-plane stiffness of these two cases is the same as case 2. In case 5, the length of slabs is equal to case 1 while the out of plane stiffness of slab is doubled.

In this paper, significant yield point is established when all reinforcement in the boundary element yield in tension or when the first boundary element in the mathematical model reached yielding state The numerical analyses results also are employed to address the importance of bay length as well as the flexural stiffness of slabs on the system-over strength factor.

The predicted finite element analysis and hand calculated values of the system over-strength factor (together with the error) for all cases are presented in Table 6. It demonstrates that in the few case studies examined in this paper; the overall error in estimation of over-strength values is in the range of 10-15%.

Table 6. Comparison of simplified and finite element method

Case	$\Omega_{\text{finite element}}$	Ω_{simple}	Error
1	0	0	0
2	1.91	1.70	11.5%
3	1.836	1.565	14.7%
4	1.843	1.655	10.2%
5	2.420	2.154	11.2%

Two main assumptions may alter the predicted values: (i) First, the simplified method overlooks the presence of corner columns as one of the boundary conditions around the slabs. (ii) Second, the effective width of the slabs is assumed equal to the bay length in the proposed equations. It seems that both assumptions are crude and they require further investigation. The equivalent slab length can be changed

to find the best agreement with finite element calculation. However, to achieve robust values for the system over-strength the different arrangement of structural walls and slabs should be represented in the model.

5. CONCLUSION

This paper has explored the effect of wall-slab-gravity system interaction on the overall behavior of shear wall building systems. It has been re-confirmed through analytical and numerical investigation that the out-of-plane stiffness of slabs can induce some additional axial forces in gravity columns and this interaction can increase the system moment capacity and the corresponding over-strength of the whole structure. In all case study buildings the system-over-strength varied from 1.91 to 2.42 due to presence of slabs. However, it was also demonstrated that doubling the out-of-plane stiffness of slabs can increase the system over-strength by 27% . However, change in the bay length from 6 m to 8 m in any direction would reduce the system-over strength by only 5 %. It seems that value of Ω mostly depends on the flexural stiffness of the slabs to a large extent and bay length, to a small extent. This system interaction effect requires additional allowance in base shear demand calculation and shear force envelope proposed for the structural walls.

REFERENCES

Aktan, Ahmet, E. & Vitelmo, V. Bertero. (1984). Seismic response of R/C frame-wall structures. Journal of Structural Engineering, 110.8, 1803-1821.

Kabeyasawa, T., Shiohara, H., Otani, S. & Aoyama, H. (1983). Analysis of the full-scale seven-story reinforced concrete test structure. Journal of the Faculty of Engineering, 37(2), 431-478.

Mander, J.B., Priestley, M.J. & Park, R. (1988). Theoretical stress-strain model for confined concrete. Journal of structural engineering, 114(8), 1804-1826.

Panagiotou, M., Restrepo, J.I. & Conte, J.P. (2010). Shake-table test of a full-scale 7-story building slice. Phase I: Rectangular wall. Journal of Structural Engineering, 137(6), 691-704.

Park, R. (1996). Explicit incorporation of element and structure overstrength in the design process. Proceedings of the 11th WCEE. IAEE, Acapulco, Mexico, Paper, (2130).

Priestley, M.J.N. (1997). Displacement-based seismic assessment of reinforced concrete buildings. Journal of earthquake Engineering, 1.01, 157-192.

Priestley, M.J.N., Calvi, G.M. & Kowalsky, M.J. (2007). Displacement Based Seismic Design of\Structures, IUSS Press, Pavia, Italy.

SAP2000 & CSI, S. (2014). Ver. 17.1.1, integrated finite element analysis and design of structures basic analysis reference manual. Berkeley (CA, USA), Computers and Structures INC.

Standard, NZ. (2006). Concrete Structures Standard, NZS 3101. NZS.

Standard, NZ. (2004). Loading Standards, NZS1170.5 NZS.